Microwave Background Temperature at a Redshift of 6.34 from H_2O Absorption

Dominik A. Riechers, Axel Weiß, Fabian Walter,
Chris Carilli, Pierre Cox, Roberto Decarli & Roberto Neri

Nature **602**, 58-62
https://arxiv.org/abs/2202.00693

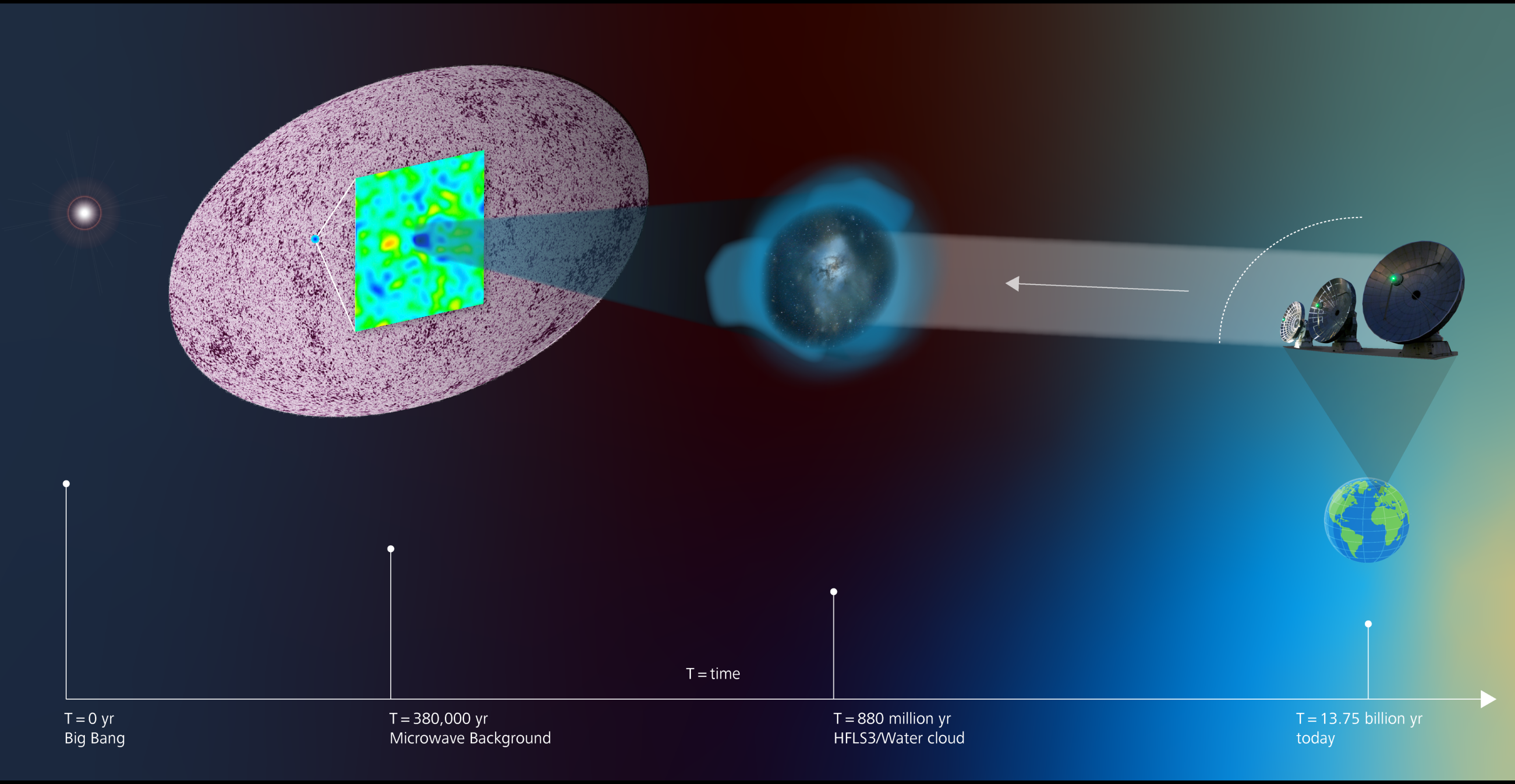

T = time
T = 0 yr
Big Bang
T = 380,000 yr
Microwave Background
T = 880 million yr
HFLS3/Water cloud
T = 13.75 billion yr
today

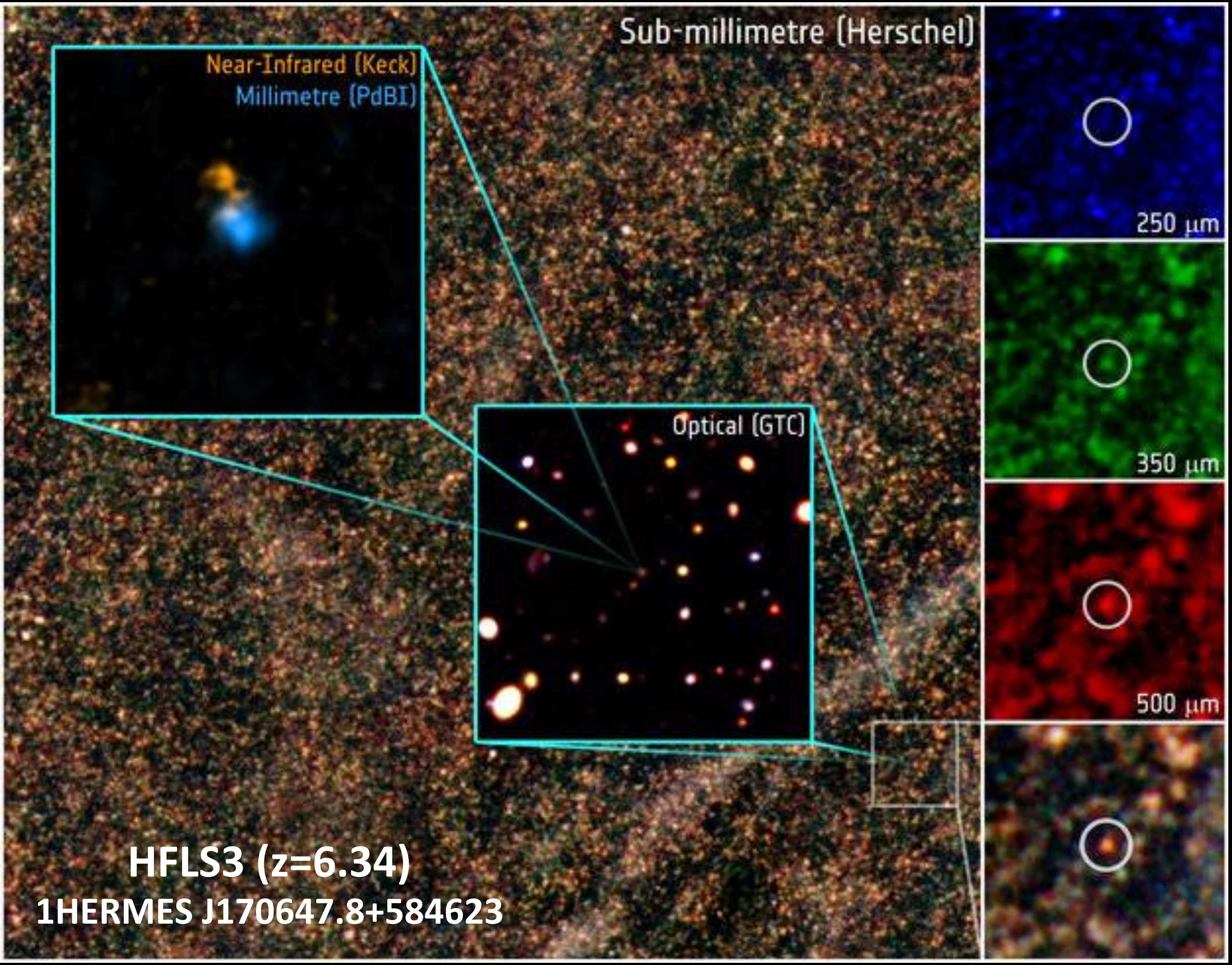
Sub-millimetre (Herschel)
Near-Infrared (Keck)
Millimetre (PdBI)
Optical (GTC)
250 μm
350 μm
500 μm
HFLS3 (z=6.34)
1HERMES J170647.8+584623

Properties of HFLS3

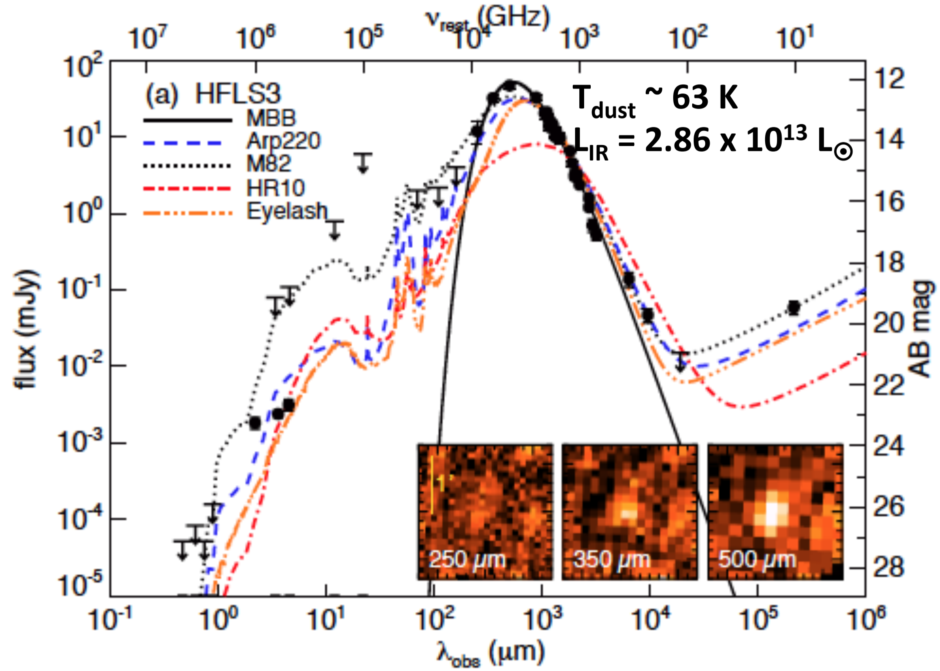

$M_{dust} = 1.3 \times 10^{9}\ M_{\odot}$
$M_{gas} = 10^{11}\ M_{\odot}$

$T_{kin} \sim 140$ K
$\log_{10}(n(H_2))=3.8\ cm^{-3}$

$M_{dyn} = 2.7 \times 10^{11}\ M_{\odot}$
$F_{gas} = M_{gas}/M_{dyn} \sim 40\%$

$SFR = 2900\ M_{\odot}\ yr^{-1}$
$t_{depl} = 36$ Myr

Size in [CII] ~ 2.6 x 2.4 kpc

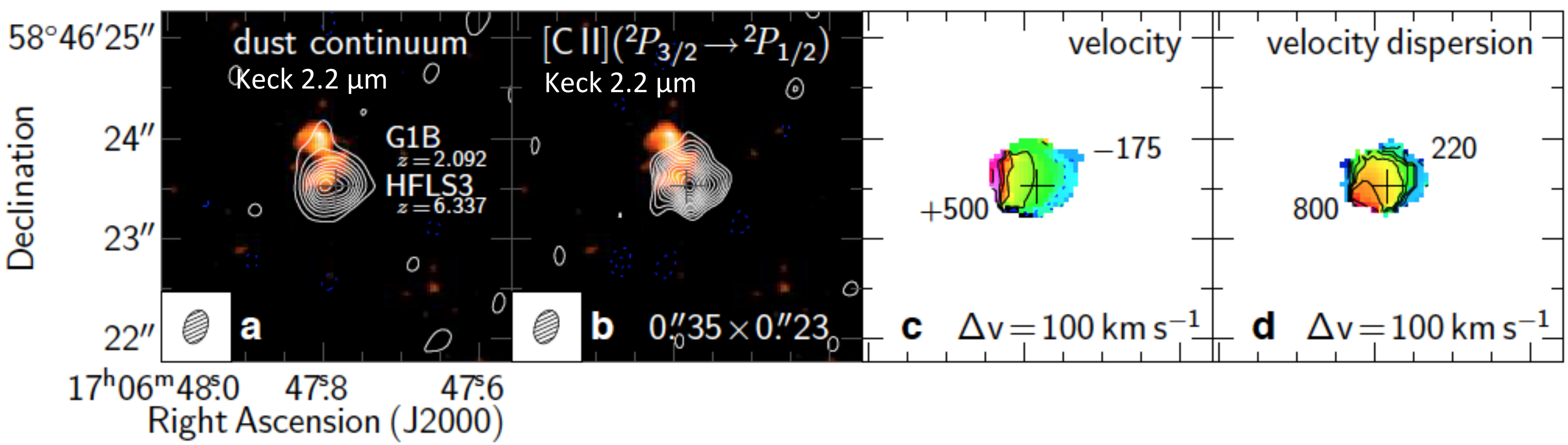

Extreme star formation rate surface density of $\Sigma_{SFR} \sim 600$ M yr^{-1} kpc^{-2} over a 1.3-kpc-radius region, consistent with near-Eddington limited star formation

Riechers et al. (2013)

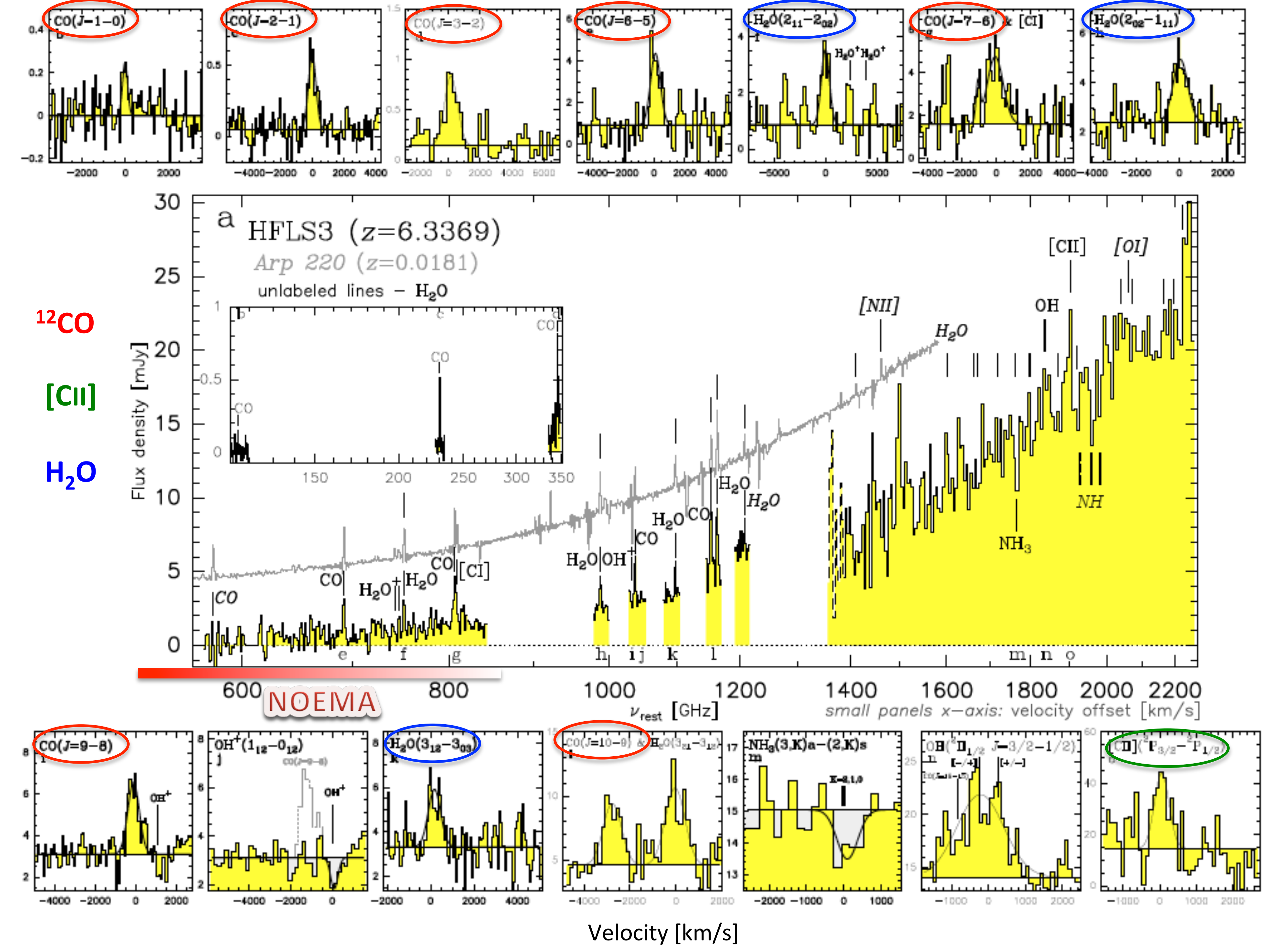

HFLS3 (z=6.3369)
Arp 220 (z=0.0181)
unlabeled lines – H2O
12CO
[CII]
H2O
Flux density [mJy]
ν_rest [GHz]
small panels x-axis: velocity offset [km/s]
NOEMA
CO(J=1–0)
CO(J=2–1)
CO(J=3–2)
CO(J=6–5)
H2O(2_11–2_02)
CO(J=7–6) & [CI]
H2O(2_02–1_11)
CO(J=9–8)
OH+(1_12–0_12)
H2O(3_12–3_03)
CO(J=10–9) & H2O(3_21–3_12)
NH3(3,K)a–(2,K)s
OH(2Π1/2 J=3/2–1/2)
[CII](2P3/2–2P1/2)
[NII]
OH
[OI]
NH3
NH
Velocity [km/s]

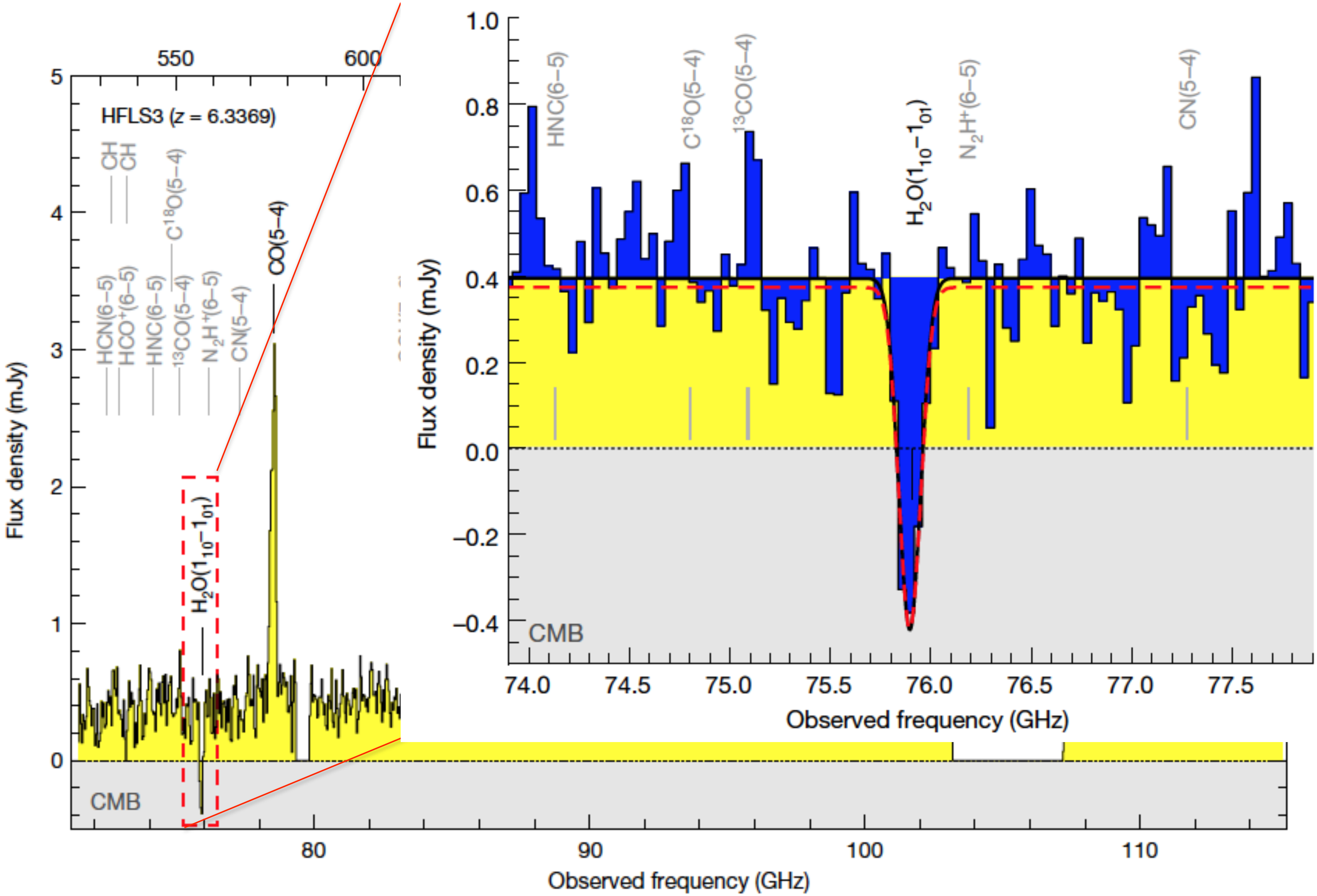

HFLS3 (z = 6.3369)
550
600
5
4
3
2
1
0
Flux density (mJy)
CH
CH
HCN(6–5)
HCO+(6–5)
HNC(6–5)
13CO(5–4)
C18O(5–4)
N2H+(6–5)
CN(5–4)
CO(5–4)
H2O(110–101)
CMB
80
90
100
110
Observed frequency (GHz)
1.0
0.8
0.6
0.4
0.2
0.0
−0.2
−0.4
HNC(6–5)
C18O(5–4)
13CO(5–4)
H2O(110–101)
N2H+(6–5)
CN(5–4)
74.0
74.5
75.0
75.5
76.0
76.5
77.0
77.5

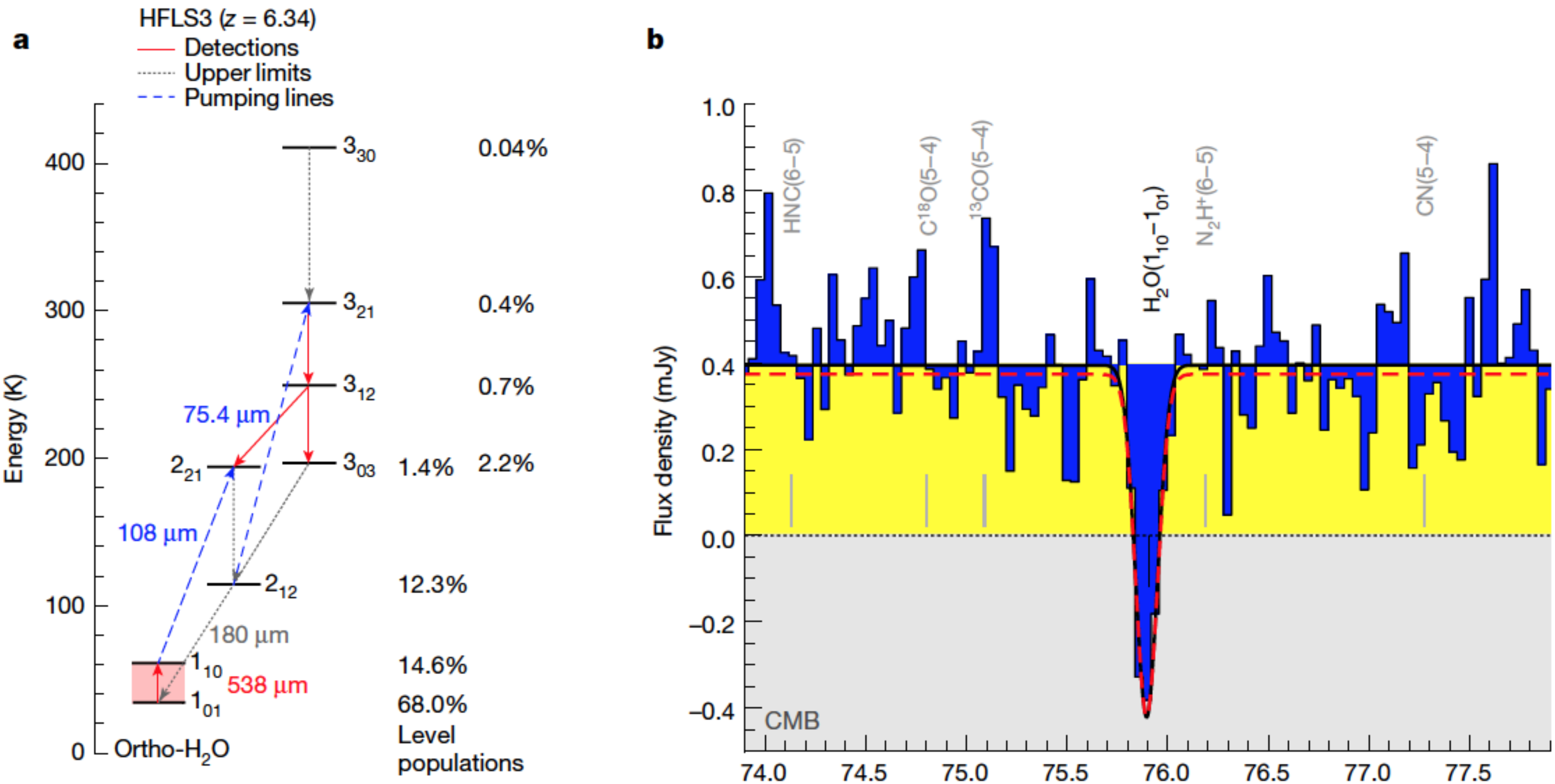

a
HFLS3 (z = 6.34)
Detections
Upper limits
Pumping lines
Energy (K)
0
100
200
300
400
3_30
3_21
3_12
3_03
2_21
2_12
1_10
1_01
0.04%
0.4%
0.7%
2.2%
1.4%
12.3%
14.6%
68.0%
Level populations
75.4 μm
108 μm
180 μm
538 μm
Ortho-H2O
b
Flux density (mJy)
Observed frequency (GHz)
1.0
0.8
0.6
0.4
0.2
0.0
−0.2
−0.4
74.0
74.5
75.0
75.5
76.0
76.5
77.0
77.5
HNC(6–5)
C18O(5–4)
13CO(5–4)
H2O(1_10–1_01)
N2H+(6–5)
CN(5–4)
CMB

Combined effect of CMB absorption and starburst radiation field on the strength of the $H_2O(1_{10}$-$1_{01})$ absorption line in HFLS3

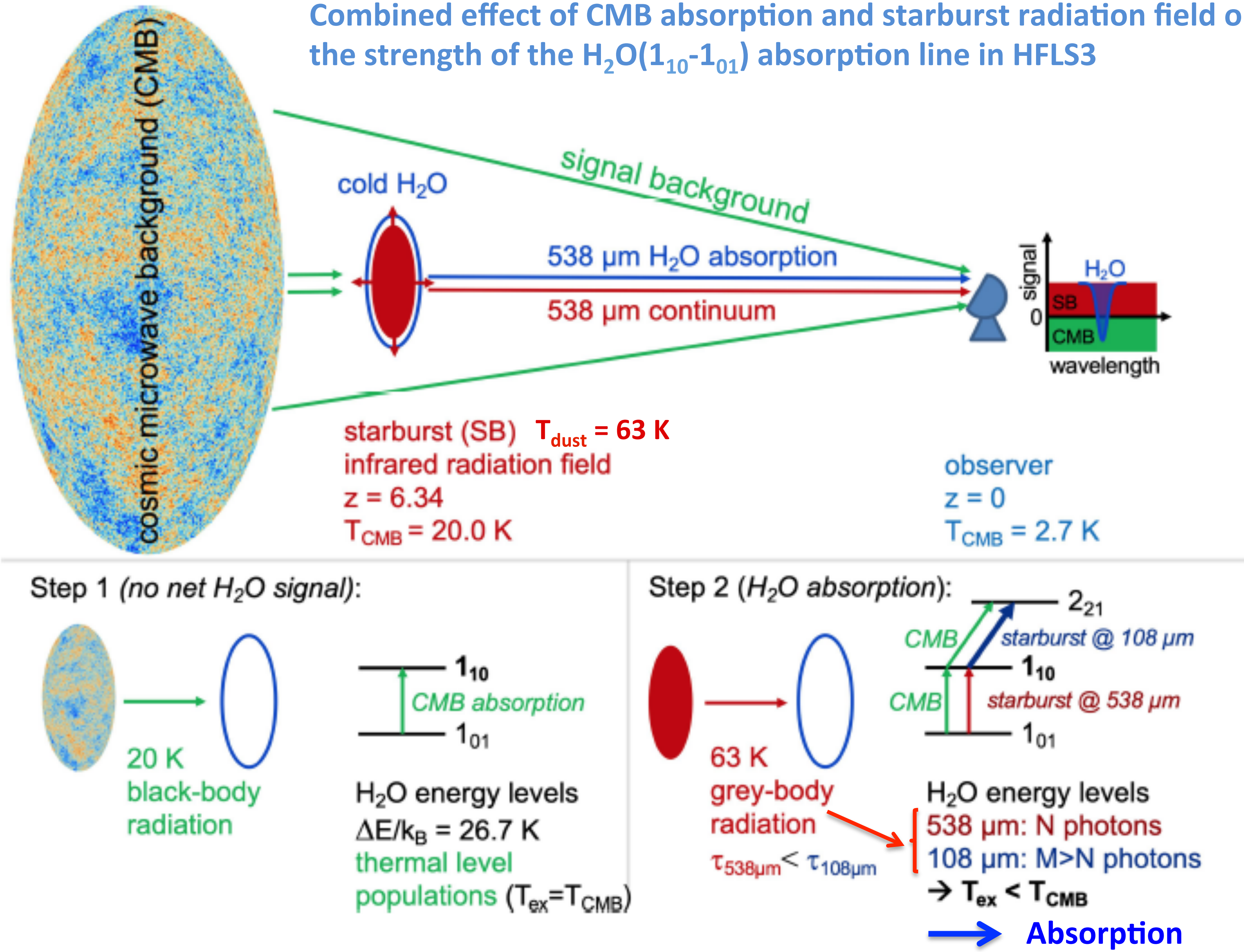

Continuum and H_2O absorption in HFLS3

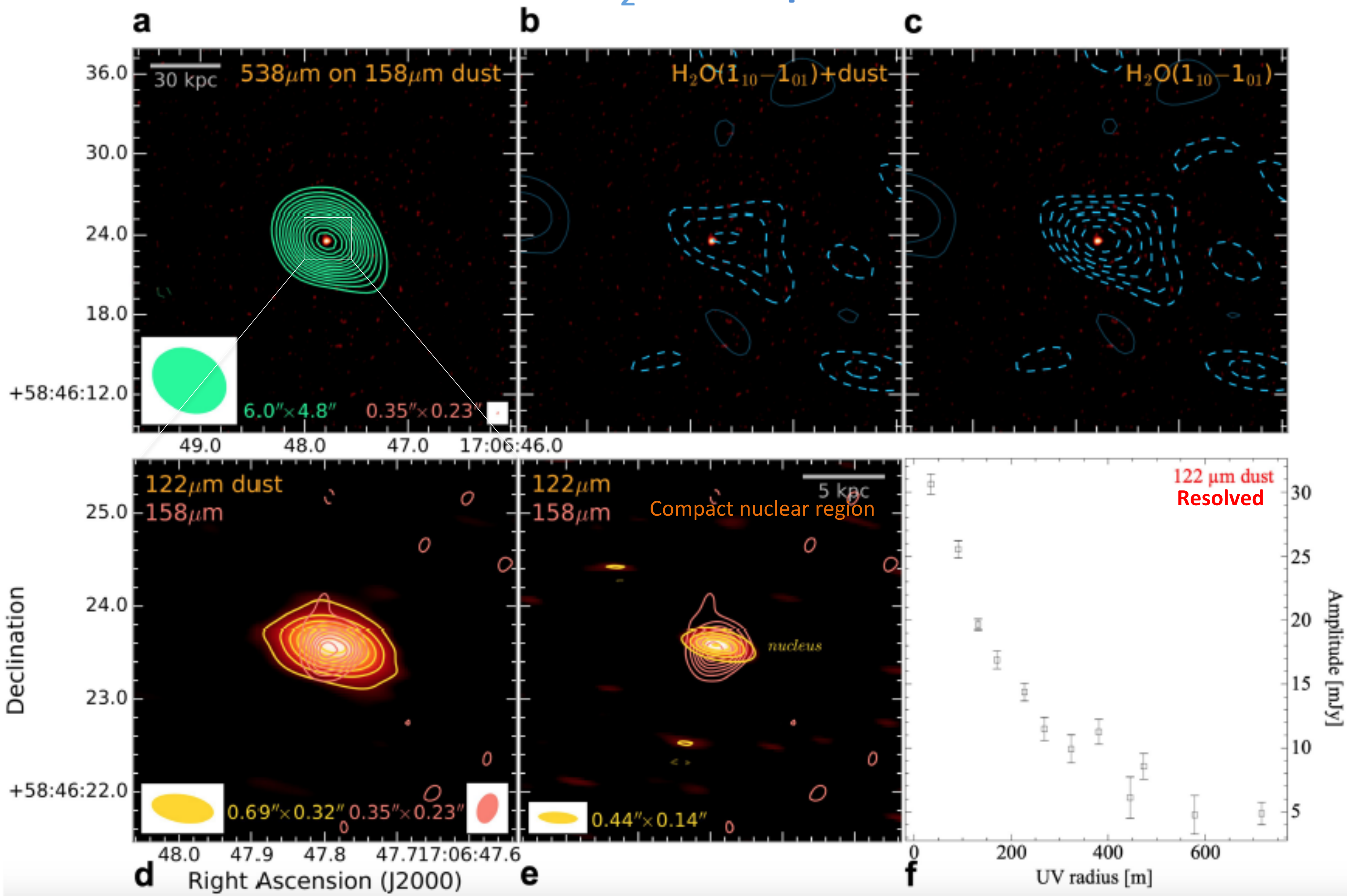

Radiative transfer models for HFLS3 and constraints on the CMB temperature

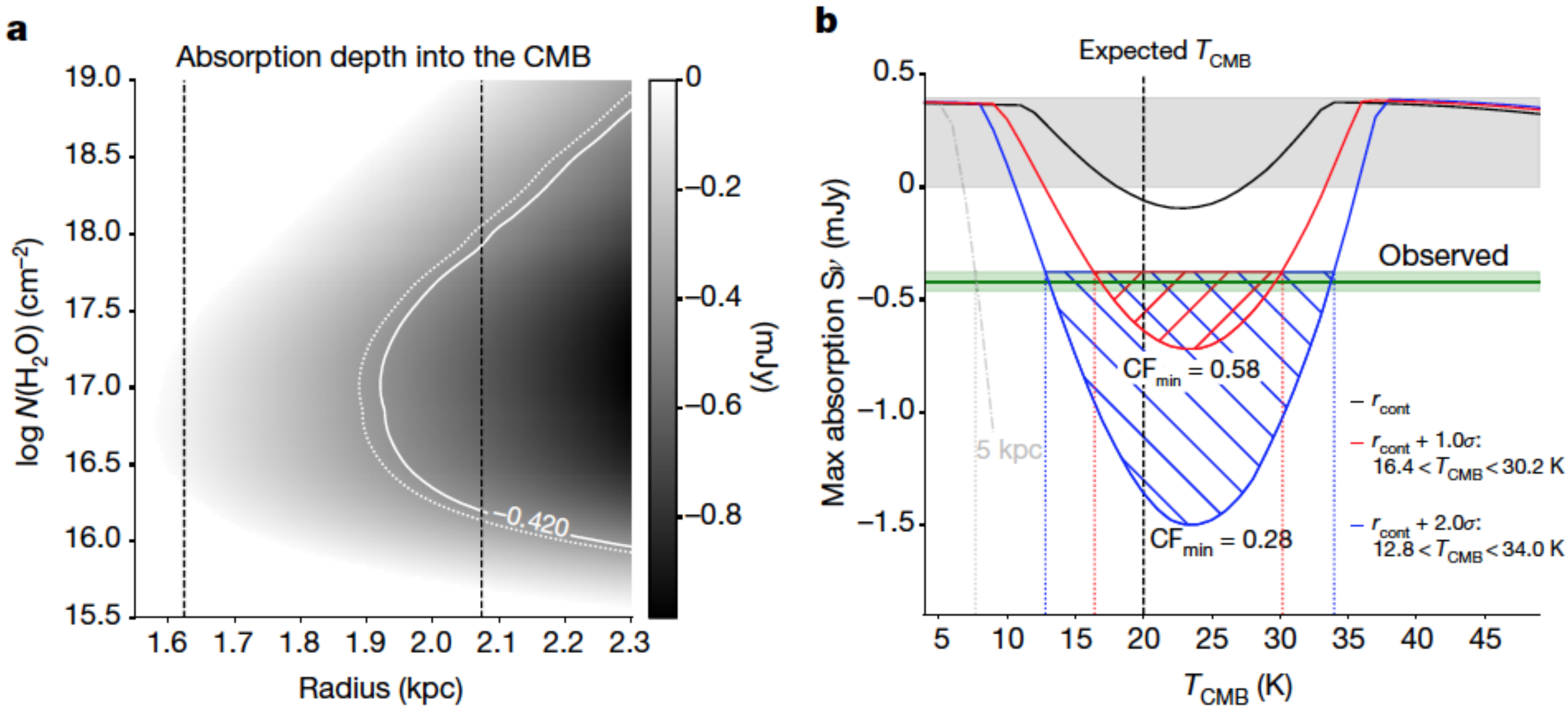

Model grid for the predicted line-absorption strength for the T_{CMB} at z=6.34 (grey scale) as a function of H_2O column density and radius of the dust-emission region at 108 µm. The white curves show the parameter space allowed by the measurements (including 1σ uncertainty region). The dashed black lines show the measured continuum size (left) and 1σ r.m.s uncertainty region. The overlapping region between the white boundary (minimum allowed absorption strength) and the size measurement (minimum required emitting area) is the allowed parameter space for the absorption strength within 1σ r.m.s.

Constraints on T_{CMB} for the observed absorption strength at the minimum size compatible with the observations (red/blue shaded regions are the allowed ranges within the sources radius +1σ/+2σ r.m.s.). The minimum filling factor of the dust emission region (CF_{min}) is indicated for the +1σ and 2σ r.m.s. regions.

Observability of the H_2O absorption as a function of redshift

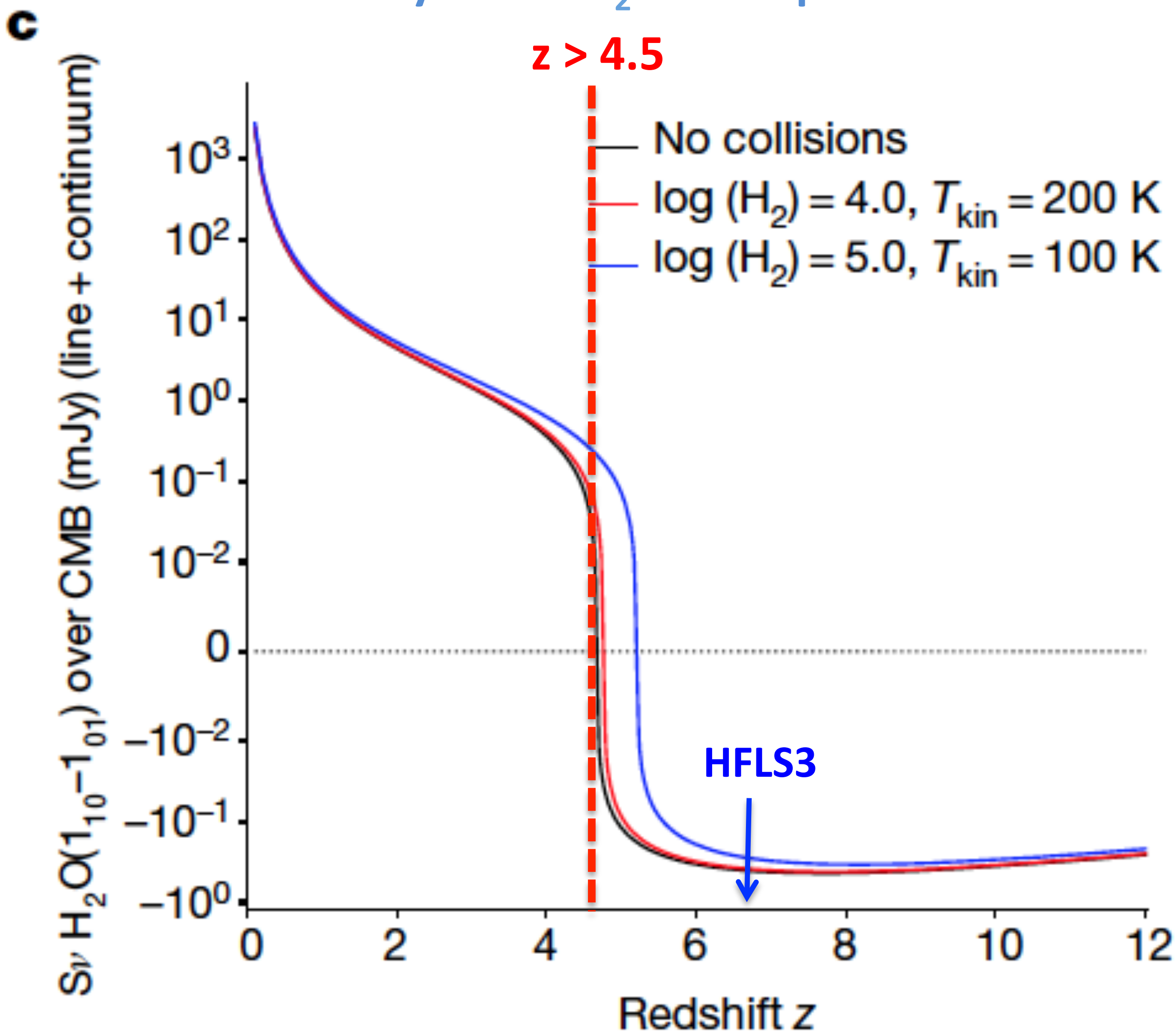

Observability of the H_2O absorption as a function of *z* for three solutions allowed by the data without and with collisional excitation. The effect becomes observable at z~4.5 and remains visible at similar strength to *z* > 12. The lower redshift limit is higher in cases where the collisional excitation is important but the impact is minor below *n*(H_2)=10^5 cm^{-3}.

$T_{CMB(z=0)}$=2.72548±0.00057 K

T_{CMB} (z=6.34) = 20.0 K

ΛCDM $T_{CMB}(z) = T_{CMB}(z=0)*(1+z)^{(1-\beta)}$

16.4 K < T_{CMB} (z=6.34) < 30.2 K

$\beta = 3.4^{+8.1}_{-7.3} \times 10^{-3}$

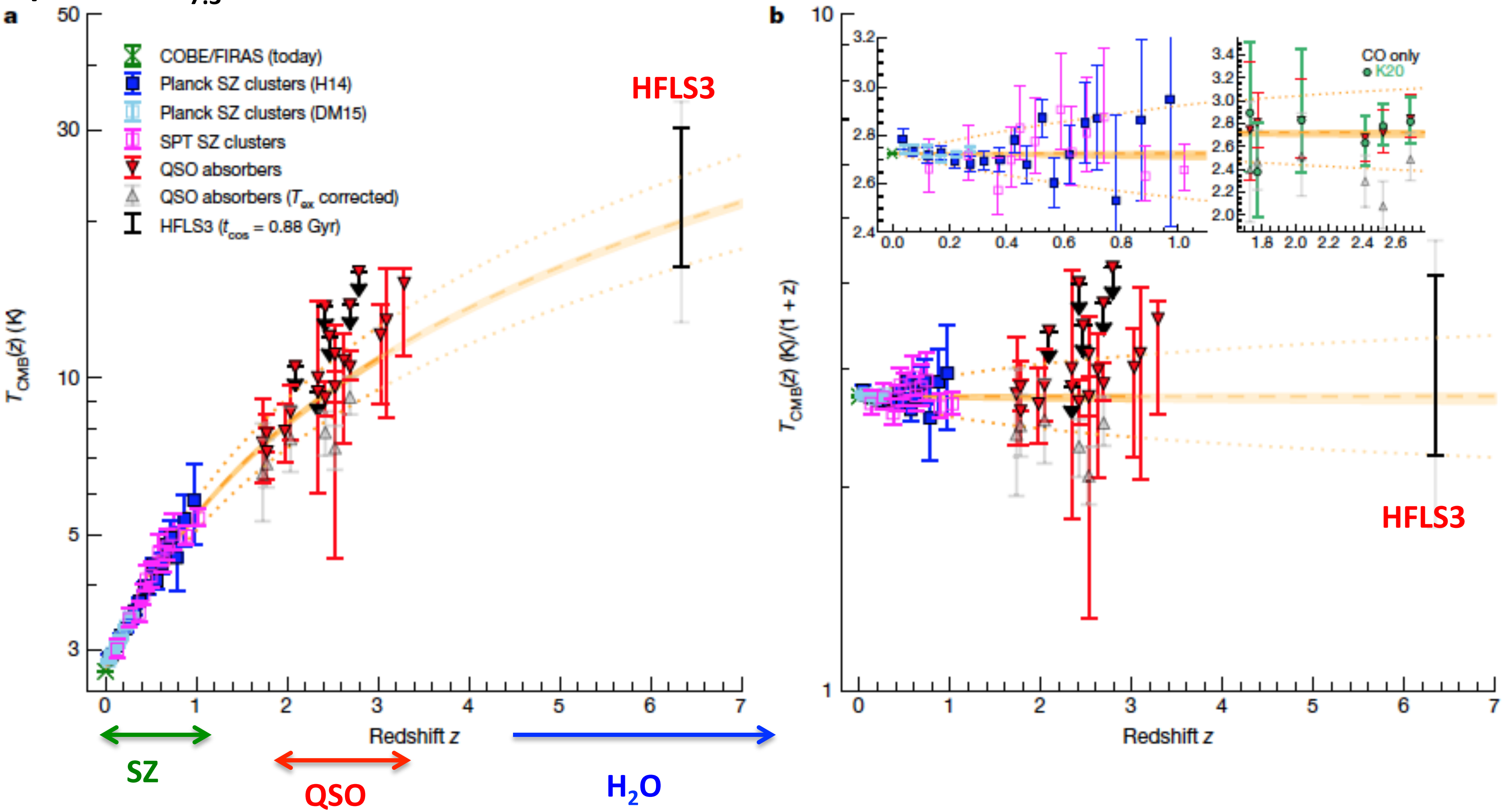

References: Sunyaev & Zel'dovich (1980); Hurier et al. (2014); Saro et al. (2014); de Martino et al. (2015); Songaila et al. (1994); Srianand, Petitjean & Ledoux (2000); Noterdaeme et al. (2011, 2017); Klimenko et al. (2020); Molaro et al. (2022)

Conclusions

- The H_2O absorption against the CMB at z=6.34 provides the most direct constraint on T_{CMB} currently available at z>4.5.
- The existence of this effect on its own directly implies that the CMB at z>4.5 is warmer than at low redshifts because T_{CMB} must be sufficiently high to notably excite the H_2O 1_{01} level, which lies 26.7 K above ground, as a basis for the observed decrement due to the de-population of this level by the starburst radiation field.
- The combined fit to the available data is consistent with the redshift scaling expected from ΛCDM.
- The derived adiabatic index γ (between pressure and energy density) fits the standard value γ=4/3 expected in ΛCDM and the effective dark energy equation of state parameter (w_{eff}= $-1.011^{+0.018}_{-0.017}$) is consistent with the w=-1 expectation for a dark energy that does not evolve with time
- Observations of the $H_2O(1_{10}-1_{01})$ absorption towards other z>4.5 starburst galaxies are on-going with the goal to measure T_{CMB} across cosmic time.